Sensors and Materials, Vol. 36, No. 2 (2024) 597–605
MYU Tokyo

S & M 3549

Radio-photoluminescence Properties of Sm-doped HfO_2–Al_2O_3–SiO_2 Glass Ceramics

Akihiro Nishikawa,[1*] Daiki Shiratori,[2] Takumi Kato,[1]
Daisuke Nakauchi,[1] Noriaki Kawaguchi,[1] and Takayuki Yanagida[1]

[1]Nara Institute of Science and Technology, 8916-5 Takayama, Ikoma, Nara 630-0192, Japan
[2]Tokyo University of Science, 6-3-1 Niijuku, Katsushika-ku, Tokyo 125-8585, Japan

(Received October 19, 2023; accepted January 11, 2024)

Keywords: glass ceramics, X-ray imaging, radio-photoluminescence, Sm

In this study, Sm-doped HfO_2–Al_2O_3–SiO_2 glass ceramics with different Sm concentrations (0.1, 0.3, 1.0, and 3.0%) were synthesized by the melt quenching method using a floating zone (FZ) furnace. Their photoluminescence properties, including radio-photoluminescence and spatial resolution, were investigated. The 0.1 and 0.3% Sm-doped samples indicated the luminescence of Sm^{3+}, and the 1.0% Sm-doped sample showed the luminescence of Sm^{2+} and Sm^{3+}. Alternatively, the 3.0% Sm-doped sample mainly showed the luminescence of Sm^{2+}. The radio-photoluminescence phenomenon ($Sm^{3+} \rightarrow Sm^{2+}$) was observed in the 0.1–1.0% Sm-doped samples. In addition, the 1.0% Sm-doped sample had a spatial resolution of 10 LP/mm.

1. Introduction

Various inorganic phosphors have been investigated for radiation measurements,[1,2] and radio-photoluminescence (RPL) materials are one of such phosphors used for dosimetry.[3–7] RPL is photoluminescence (PL) that occurs through luminescence centers generated by X-ray irradiation. The amount of luminescence centers is proportional to the irradiation dose; thus, measuring the luminescence intensity can estimate the irradiation dose. The Ag-doped phosphate glass is a common RPL material.[8] The RPL center of this material is Ag^{2+}. Before X-ray irradiation to the Ag-doped phosphate glass, most Ag exists as Ag^{+} in the glass matrix. Then, Ag^{+} changes to Ag^{2+} with X-ray irradiation.[9] In this case, Ag^{2+} is stable at room temperature in the glass matrix, so the luminescence intensity of Ag^{2+} can be observed repeatedly. In other words, once dose information is stored by the Ag-doped phosphate glass, we can read out the dose information repeatedly without losing it.

RPL materials are used primarily for personal dosimetry, but an X-ray imaging plate (IP) using RPL has been considered.[10,11] Currently, optically stimulated luminescence (OSL) materials are typically used as phosphors for IP;[12–15] however, the stored OSL signal is reduced by the laser during readout. When OSL materials are read out with strong excitation light, the readout and unintended points are excited simultaneously, resulting in a decrease in OSL

*Corresponding author: e-mail: nishikawa.akihiro.nc6@ms.naist.jp
https://doi.org/10.18494/SAM4755

ISSN 0914-4935

intensity and resolution. On the other hand, RPL has the potential to solve the problem and even achieve a high resolution by combining confocal laser scanning microscopy. Thus, we focused on developing new RPL materials to replace the OSL materials in IP applications.

In this study, Sm-doped HfO_2–Al_2O_3–SiO_2 glass ceramics were prepared by the melt quenching method using an optical floating zone (FZ) furnace, and their PL and RPL properties and spatial resolutions were investigated. The commercial RPL material used for personal dosimetry has as low effective atomic number (Z_{eff}) as human tissues. However, we aim to develop RPL materials for IP, so materials with high Z_{eff} are preferred to increase the interaction probability of X-rays. Thus, HfO_2 was chosen to increase the Z_{eff} of the host material. In addition, Sm was selected as an RPL center. Sm was reported to indicate the RPL phenomenon, in which Sm^{3+} changes to Sm^{2+} through ionizing radiation.[16–19]

2. Materials and Methods

2.1 Sample preparation

Sm-doped $10HfO_2$-$10Al_2O_3$-$80SiO_2$ glass ceramics were synthesized by the melt quenching method using an optical FZ furnace. HfO_2 has a high melting point; thus, we applied the optical FZ furnace, not an electric furnace, to prepare the glasses. The starting materials of the host glass, namely, HfO_2 (4N), Al_2O_3 (4N), and SiO_2 (4N) powders, were uniformly mixed at a molar ratio of 10:10:80, respectively. This host glass has a Z_{eff} of 45. Sm_2O_3 (4N) was added to the host glass with concentrations of 0.1, 0.3, 1.0, and 3.0 mol.%. Four grams in total of these powders was mixed in an agate mortar. The mixed powders were formed into a cylinder rod using hydrostatic pressure, and this rod was sintered at 1200 ℃ for 8 h in air. The optical FZ furnace (FZ-T-12000-X-VPO-PC-Y, Crystal Systems), which can achieve a temperature of approximately 3000 ℃, melted the obtained ceramic rod with four Xe lamps. In addition, the molten part was dropped into the water and rapidly quenched. The glass sample obtained by this method has a spherical morphology with a diameter of less than 10 mm. The obtained glass samples were mechanically polished.

2.2 Measurement method

X-ray diffraction (XRD) measurements were conducted to confirm the amorphous phase of the samples. XRD patterns were measured using MiniFlex 600 (RIGAKU). Diffuse transmittance spectra were measured with a spectrophotometer (SolidSpec-3700, Shimadzu). The absorption spectra in the infrared region were also measured using a spectrophotometer (V670, JASCO), and the measurement was performed across the spectral range from 1.7 to 3.0 μm.

For the evaluation of RPL properties, the excitation and emission spectra obtained before and after X-ray irradiation were measured using a spectrofluorometer (FP-8600, JASCO). The measurement interval was 1 nm. Moreover, the PL lifetimes of the samples observed before and after X-ray irradiation were measured using Quantaurus-Tau (C11367, Hamamatsu Photonics).

To expose X-rays to the samples, an X-ray generator (XRBOP&N200X4550, Spellman) was used. The samples were irradiated with 10 Gy of X-rays.

In terms of the imaging device capability, test charts (Pro-Res RF BarType7, PROPROJECT) were used to evaluate the spatial resolution. The samples were irradiated with X-rays through a test chart. Subsequently, the samples were excited with 440 nm light, and the emission through an optical filter (LV0670, Asahi Spectra) was received by a CCD camera (BU-54UV, Bitran) to obtain X-ray images.

3. Results and Discussion

Figure 1(a) shows the appearance of all samples. All samples were approximately 6 mm in diameter, 1.1 mm thick, and transparent, but the 3.0% Sm-doped sample was reddish. Figure 1(b) shows the XRD patterns of all the samples, and broad and sharp peaks were observed. The broad peak at 25 degrees was regarded as the halo peak, which was generally observed in amorphous materials, while the sharp peaks at 30, 35, 50, and 60 degrees were suitable for cubic-HfO_2 (c-HfO_2) (space group: Fm-3m, PDF: 00-053-0550) crystal peaks. These peaks were also observed in the undoped $10HfO_2$–$10Al_2O_3$–$80SiO_2$ glass.[20] It was found that all the samples were glass ceramics, including the c-HfO_2 phase without lost transparency.

Figure 2(a) shows the diffuse transmittance spectra of all the samples. The 0.1, 0.3, and 1.0% Sm-doped samples indicated an absorption band at around 200–300 nm. This absorption band was attributed to the absorption of undoped HfO_2–Al_2O_3–SiO_2 glass ceramics.[20] In addition, a sharp absorption at around 400 nm in the 0.1–1.0% Sm-doped samples and an absorption band at around 300–450 nm in the 3.0% Sm-doped sample were observed. The absorption peaks at around 400 nm were attributed to the 4*f*–4*f* transition of Sm^{3+}.[21–23] The absorption band at around 300–450 nm in the 3.0% Sm-doped sample would be related to the 4*f*–5*d* transition of Sm^{2+}. Figure 2(b) shows the absorption spectrum of the 1.0% Sm-doped sample in the infrared region. This absorption spectrum was measured to confirm the presence or absence of the OH group in the sample because of the use of water in the synthesis process. Since the same absorption band was obtained for all the samples, the absorption spectrum of the 1.0% Sm-doped sample is shown as a representative. Absorption bands for OH groups are generally observed at 1.91, 2.22, and 2.52 μm in silicate glass.[24] Such absorption bands were observed in the 1.0% Sm-doped sample. The presence of OH groups in the samples might be due to the effect of using water for quenching.

Figure 3(a) shows the PL excitation and emission spectra of the 3.0% Sm-doped sample. Excitation peaks at around 340, 360, and 400 nm under monitoring at 600 nm were attributed to transitions of $^6H_{5/2} \rightarrow {}^4H_{9/2}$, $^6P_{7/2}$, and $^4F_{7/2}$.[25] The excitation peaks monitored at 690 nm emission were detected at around 350 and 440 nm, which were attributed to the $4f^6$–$4f^5$–$5d^1$ transition.[26] There were emission peaks at around 560, 600, 650, 690, 710, and 730 nm under 400 nm excitation. On the other hand, the emission peaks were mainly observed at around 690 and 730 nm under 440 nm excitation. Figure 3(b) shows the PL decay curves of all the samples when the emission wavelength is monitored at 600 nm. The decay curve of the 0.1% Sm-doped sample was approximated by two exponential decay components, and the decay curves of the

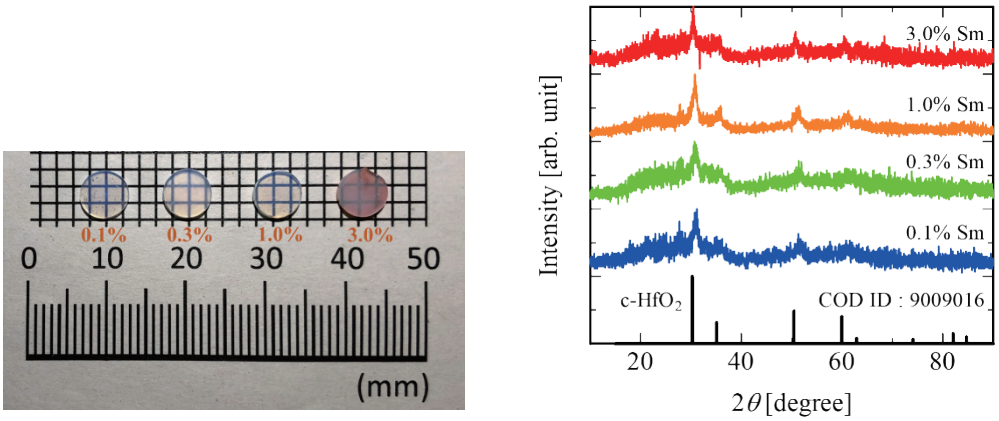

(a) (b)

Fig. 1. (Color online) (a) Appearance and (b) XRD patterns of all samples.

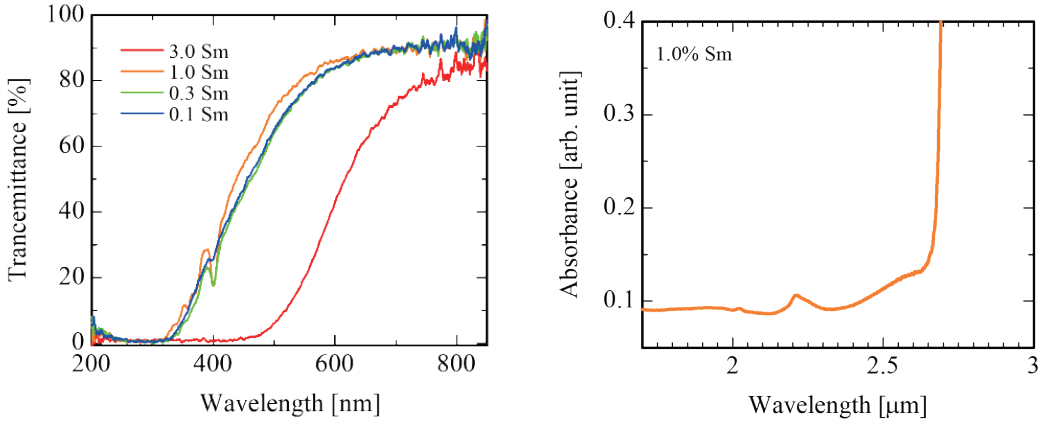

(a) (b)

Fig. 2. (Color online) (a) Diffuse transmittance spectra of all samples and (b) absorption spectrum of 1.0% Sm-doped sample in infrared region.

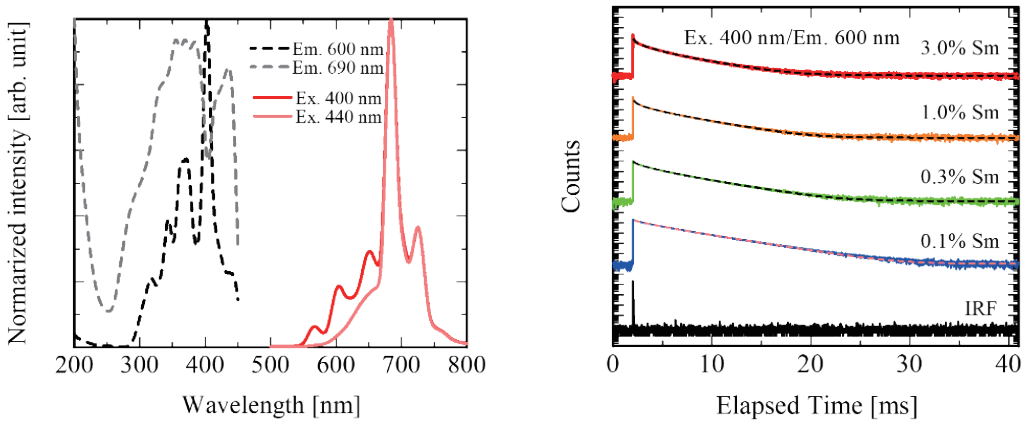

(a) (b)

Fig. 3. (Color online) (a) PL excitation and emission spectra of 3.0% Sm-doped sample; dashed lines show excitation spectra and solid lines show emission spectra. (b) PL decay curves of all samples. Instrument Response Function (IRF) is excitation light leakage.

other samples were approximated by three ones. The calculated lifetimes are shown in Table 1. The lifetimes of the 0.1% Sm-doped sample were 1.29 and 2.89 ms, which would be attributed to Sm^{3+}.[27] In the other samples, PL lifetimes of 169–283 μs and 1.01–2.77 ms were observed. The first component was assigned to Sm^{2+},[28] and the second and third ones would be attributed to Sm^{3+} as well as the 0.1% Sm-doped sample. On the basis of these emission wavelengths and lifetimes, the emission peaks at around 560, 600, 650, and 710 nm were found to originate from the $^4G_{5/2} \rightarrow {}^6H_{5/2}$, $^6H_{7/2}$, $^6H_{9/2}$, and $^6H_{11/2}$ transitions of Sm^{3+}, and the emission peaks at around 690 and 730 nm originated from the $^5D_0 \rightarrow {}^7F_0$ and $^7F_2$ transitions of Sm^{2+}, respectively.[29–31]

Figure 4 shows the PL emission spectra of all the samples obtained before and after X-ray irradiation. Before X-ray irradiation, the 0.1 and 0.3% Sm-doped samples showed the luminescence of Sm^{3+} (560, 600, 650, and 710 nm), and the 1.0% Sm-doped sample indicated the luminescence of Sm^{2+} (690 and 730 nm) and Sm^{3+}. On the other hand, the 3.0% Sm-doped sample before X-ray irradiation mainly exhibited the luminescence of Sm^{2+}. After X-ray irradiation, the decrease in Sm^{3+} emission intensity and the increase in Sm^{2+} emission intensity were observed in the 0.1–1.0% Sm-doped samples, and the 3.0% Sm-doped sample did not show significant changes. These results are based on the valence change ($Sm^{3+} \rightarrow Sm^{2+}$) caused by X-ray irradiation.[18] In other words, the 0.1–1.0% Sm-doped samples indicated the RPL phenomenon.

Figure 5 shows the dose response function of the 1.0% Sm-doped sample. The 1.0% Sm-doped sample exhibited the dose response function with a good linear relationship in the range of 1–30 Gy, and this result supported the fact that Sm^{2+} was formed by irradiation.

Figure 6(a) shows the repeated measurement of the RPL intensity of the 1.0% Sm-doped sample. The plots indicated the difference in RPL intensity at 690 nm before and after X-ray irradiation with normalization by the first measurement intensity. The reset was conducted by annealing at 500 °C for 1 h. No significant change in RPL intensity with the number of measurements was observed, suggesting the reusability of the samples. Figure 6(b) shows the change in RPL intensity with elapsed time. Here, the intensity was normalized at the first day. The RPL intensity increased one day after X-ray irradiation, suggesting that a buildup phenomenon had occurred, and it monotonically decreased after the second day.

The X-ray imaging test was conducted using the 1.0% Sm-doped sample because of the high emission intensity of Sm^{2+} after X-ray irradiation. Figure 7 shows the image obtained by the X-ray imaging test. The spatial resolution was evaluated using the reciprocal of the width of a line pair that could be considered resolved on the image. As a result, the spatial resolution was 10 LP/mm.

Table 1
PL lifetimes of all samples.

Sample	Lifetime (ms)		
	1st	2nd	3rd
0.1	1.29	2.89	N/A
0.3	0.283	1.29	2.77
1.0	0.221	1.03	2.60
3.0	0.169	1.01	2.62

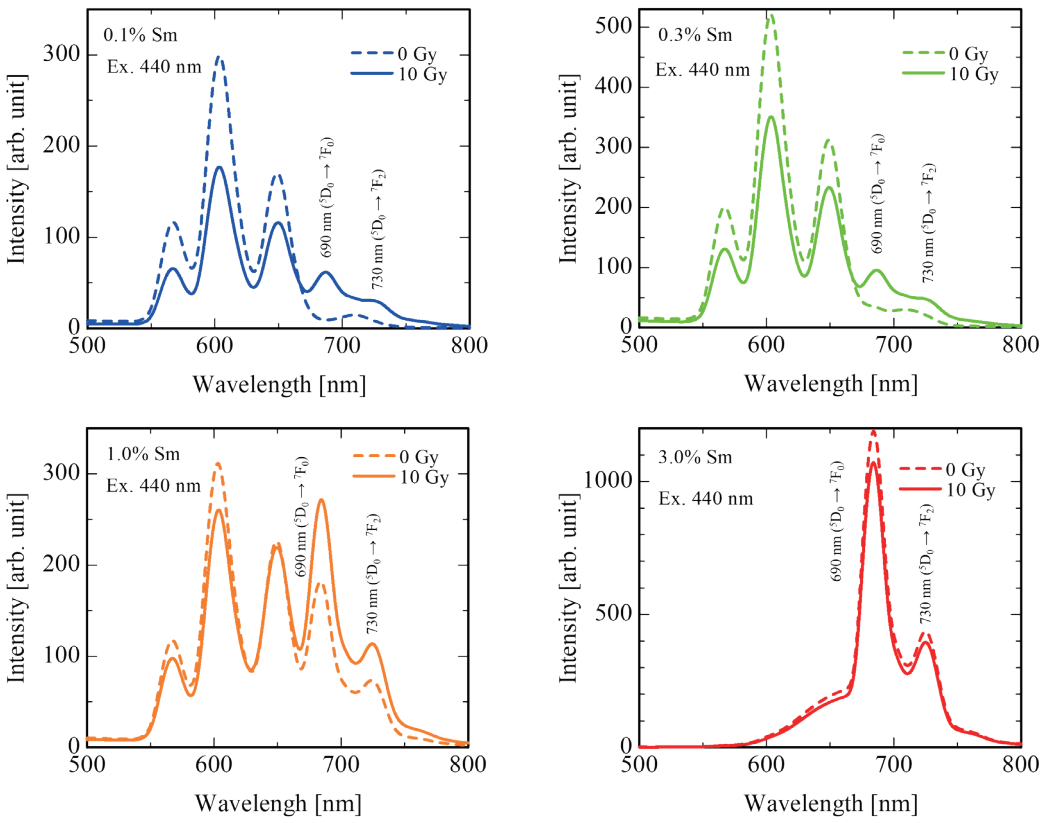

Fig. 4. (Color online) (Clockwise from the top left) PL emission spectra of 0.1, 0.3, 1.0, and 3.0% Sm-doped samples obtained before and after X-ray irradiation. The irradiation dose is 10 Gy.

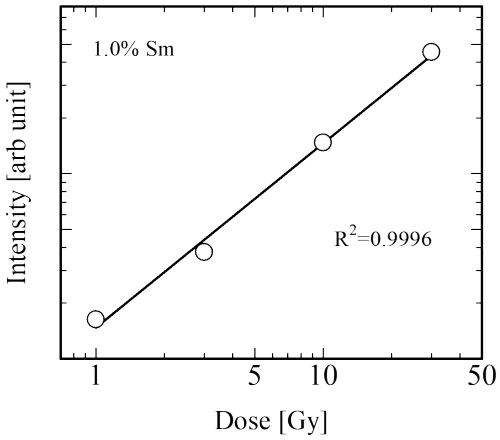

Fig. 5. Dose response function of 1.0% Sm-doped sample.

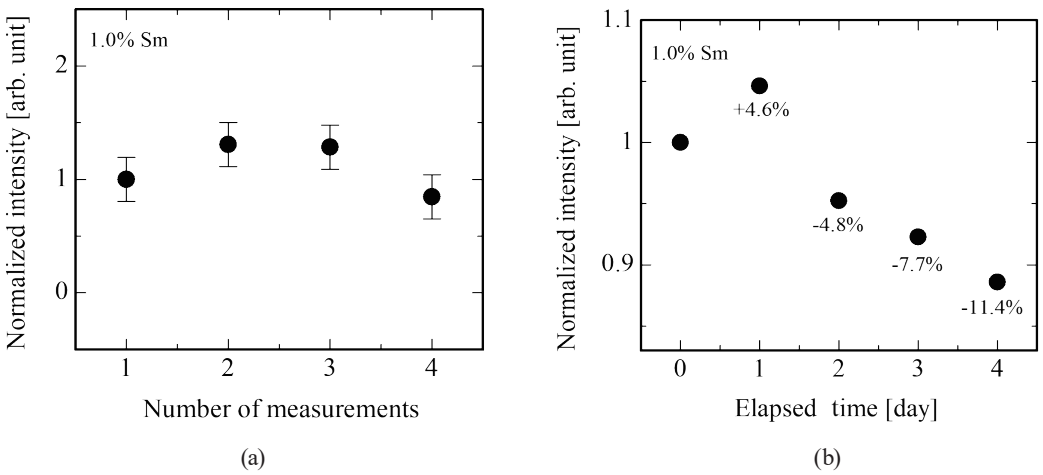

Fig. 6. (a) Repeated measurement of RPL intensity of 1.0% Sm-doped sample and (b) change in RPL intensity with elapsed time.

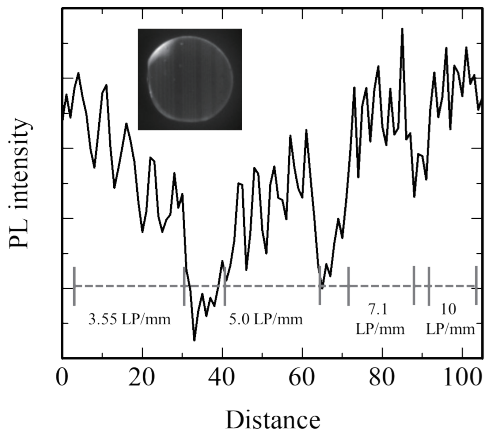

Fig. 7. Image of 1.0% Sm-doped sample obtained by an X-ray imaging test and its luminance intensity.

4. Conclusion

Sm-doped HfO_2–Al_2O_3–SiO_2 glass ceramics were prepared successfully; however, the glasses included the crystalline phase of c-HfO_2. The glasses were transparent despite the inclusion of the crystalline phase. Their PL properties were evaluated using a 3.0% Sm-doped sample. PL emission peaks were detected at around 560, 600, 650, 690, 710, and 730 nm under 400 and 440 nm excitations. The peaks at around 560, 600, 650, and 710 nm were due to the 4*f*–4*f* transition of Sm^{3+}. On the other hand, the peaks at around 690 and 730 nm were attributed to the 4*f*–4*f* transition of Sm^{2+}. Before X-ray irradiation, the 0.1 and 0.3% Sm-doped samples indicated only the Sm^{3+} luminescence, and the 1.0 and 3.0% Sm-doped samples indicated the Sm^{2+} and Sm^{3+} luminescence. The emission intensity of the 0.1–1.0% Sm-doped samples was changed by X-ray irradiation, in which the Sm^{2+} emission intensity increased with decreasing

Sm^{3+} emission intensity. This confirmed the existence of the RPL phenomenon. The X-ray imaging test was conducted using the 1.0% Sm-doped sample. The result was that it had a spatial resolution of 10 LP/mm.

Acknowledgments

This work was supported by Grants-in-Aid for Scientific Research A (22H00309), Scientific Research B (22H03872, 22H02939, 21H03733, and 21H03736), Early-Career Scientists (23K13689), and Challenging Exploratory Research (22K18997) from the Japan Society for the Promotion of Science. The Cooperative Research Project of the Research Center for Biomedical Engineering, Nippon Sheet Glass Foundation, Terumo Life Science Foundation, KRF Foundation, Tokuyama Science Foundation, Iketani Science and Technology Foundation, and Foundation for Nara Institute of Science and Technology are also acknowledged.

References

1 T. Yanagida, T. Kato, D. Nakauchi, and N. Kawaguchi: Sens. Mater. **34** (2022) 595. https://doi.org/10.18494/SAM3684
2 M. Koshimizu, S. Kurashima, A. Kimura, M. Taguchi, T. Yanagida, Y. Fujimoto, and K. Asai: Sens. Mater. **34** (2022) 637. https://doi.org/10.18494/SAM3694
3 T. Yanagida, G. Okada, T. Kato, D. Nakauchi, and N. Kawaguchi: Radiat. Meas. **158** (2022) 106847. https://doi.org/10.1016/j.radmeas.2022.106847
4 G. Okada, K. Hirasawa, T. Yanagida, and H. Nanto: Sens. Mater. **33** (2021) 2117. https://doi.org/10.18494/SAM.2021.3327
5 Ž. Knežević, N. Beck, Đ. Milković, S. Miljanić, and M. Ranogajec-Komor: Radiat. Meas. **46** (2011) 1582. https://doi.org/10.1016/j.radmeas.2011.05.042
6 T. Yanagida: Proc. Japan Acad. Ser. B **94** (2018) 75. https://doi.org/10.2183/pjab.94.007
7 G. Okada, Y. Koguchi, T. Yanagida, S. Kasap, and H. Nanto: Jpn. J. Appl. Phys. **62** (2023) 010609. https://doi.org/10.35848/1347-4065/ac9023
8 Y. C. David and S.-M. Hsu: in Adv. Cancer Ther. (InTech, 2011). https://doi.org/10.5772/23710
9 H. Kawamoto, M. Koshimizu, Y. Fujimoto, and K. Asai: Jpn. J. Appl. Phys. **62** (2023) 010501. https://doi.org/10.35848/1347-4065/ac9cb0
10 A. Edgar, C. R. Varoy, C. Koughia, G. Okada, G. Belev, and S. Kasap: J. Non-Cryst. Solids **377** (2013) 124. https://doi.org/10.1016/j.jnoncrysol.2012.12.022
11 D. Shiratori, Y. Takebuchi, T. Kato, D. Nakauchi, N. Kawaguchi, and T. Yanagida: Sens. Mater. **34** (2022) 745. https://doi.org/10.18494/SAM3695
12 H. Li, P. Hackenschmied, E. Epelbaum, and M. Batentschuk: Mater. Sci. Eng., B **94** (2002) 32. https://doi.org/10.1016/S0921-5107(02)00068-5
13 R. H. Templer: Nucl. Instrum. Methods Phys. Res., Sect. B **300** (1991) 357. https://doi.org/10.1016/0168-9002(91)90449-Z
14 M. Batentschuk, A. Winnacker, K. Schwartz, and C. Trautmann: J. Lumin. **125** (2007) 40. https://doi.org/10.1016/j.jlumin.2006.08.023
15 Y. Iwabuchi, N. Mori, K. Takahashi, T. Matsuda, and S. Shionoya: Jpn. J. Appl. Phys. **33** (1994) 178. https://doi.org/10.1143/JJAP.33.178
16 G. Okada, K. Hirasawa, E. Kusano, T. Yanagida, and H. Nanto: Nucl. Instrum. Methods Phys. Res., Sect. B **466** (2020) 56. https://doi.org/10.1016/j.nimb.2020.01.020
17 J. J. Schuyt and G. V. M. Williams: Mater. Res. Bull. **106** (2018) 455. https://doi.org/10.1016/j.materresbull.2018.06.039
18 G. Okada, K. Shinozaki, T. Komatsu, S. Kasap, and T. Yanagida: Radiat. Meas. **106** (2017) 73. https://doi.org/10.1016/j.radmeas.2016.12.006
19 K. Ichiba, G. Okada, Y. Takebuchi, T. Kato, D. Shiratori, D. Nakauchi, N. Kawaguchi, and T. Yanagida: J. Lumin. **257** (2023) 119698. https://doi.org/10.1016/j.jlumin.2023.119698

20 D. Shiratori, H. Fukushima, D. Nakauchi, T. Kato, N. Kawaguchi, and T. Yanagida: Jpn. J. Appl. Phys. **62** (2023) 010608. https://doi.org/10.35848/1347-4065/ac90a4
21 H. Lin, D. Yang, G. Liu, T. Ma, B. Zhai, Q. An, J. Yu, X. Wang, X. Liu, and E. Yue-Bun Pun: J. Lumin. **113** (2005) 121. https://doi.org/10.1016/j.jlumin.2004.09.115
22 C. Madhukar Reddy, G. R. Dillip, K. Mallikarjuna, S. Zulifiqar Ali Ahamed, B. Sudhakar Reddy, and B. Deva Prasad Raju: J. Lumin. **131** (2011) 1368. https://doi.org/10.1016/j.jlumin.2011.03.016
23 L. C. Dixie, A. Edgar, and M. F. Reid: J. Lumin. **132** (2012) 2775. https://doi.org/10.1016/j.jlumin.2012.05.026
24 E. Stolper: Contrib. to Mineral. Petrol. **81** (1982) 1. https://doi.org/10.1007/BF00371154
25 Y. Tayal and A. S. Rao: Opt. Mater. **107** (2020) 110070. https://doi.org/10.1016/j.optmat.2020.110070
26 Q. Zeng, N. Kilah, and M. Riley: J. Lumin. **101** (2003) 167. https://doi.org/10.1016/S0022-2313(02)00410-6
27 B. C. Jamalaiah, J. Suresh Kumar, A. Mohan Babu, T. Suhasini, and L. Rama Moorthy: J. Lumin. **129** (2009) 363. https://doi.org/10.1016/j.jlumin.2008.11.001
28 S. Sakirzanovas, A. Katelnikovas, D. Dutczak, A. Kareiva, and T. Jüstel: J. Lumin. **131** (2011) 2255. https://doi.org/10.1016/j.jlumin.2011.05.060
29 A. Herrmann, M. Tewelde, S. Kuhn, M. Tiegel, and C. Rüssel: J. Non-Cryst. Solids **502** (2018) 190. https://doi.org/10.1016/j.jnoncrysol.2018.09.008
30 K. Selvaraju and K. Marimuthu: J. Alloys Compd. **553** (2013) 273. https://doi.org/10.1016/j.jallcom.2012.11.150
31 J. Yang, B. Zhai, X. Zhao, Z. Wang, and H. Lin: J. Phys. Chem. Solids **74** (2013) 772. https://doi.org/10.1016/j.jpcs.2013.01.021